

Injector counter-wound solenoids have large radial gradients Rev 6

Jay Benesch

Abstract

We report here magnetic finite element modeling results on two injector magnets with drawings in Document Control, minor machining which can improve field quality by about 10%, and four new designs which provide substantially more improvement. There is a trade-off between stray field magnitude and field quality. The magnets drawn appear to have been designed for the absolute minimum of stray field with no weight given to radial gradient of B_z . The change in focusing for mm scale steering is comparable to that provided by quadrupoles in the 6 MeV region of the CEBAF injector. It is hypothesized that much of the extreme care needed during injector setup is caused by the gradients in the counter-wound solenoids.

Background

To provide information for GPT (1) particle tracking in the chopper region with three-Wien filter, the counter-wound solenoid described by drawing 39200-D-0067 has been modeled. Units of this outer envelope, 8.5" diameter by 3" long, are installed on each side of the chopping slits. These magnets are denoted MFD in the control system. No other magnets of this size were found by Document Control, but there are several magnets in the injector without easily found drawings and this may not be the installed magnet. R. Legg reports assembling several such magnets for the injector in 1993 so units with this design philosophy are installed before the quarter cryomodule. All but one of these are in the 100/130 keV region. The last is at 500 keV after the capture cavity.

Document Control also provided drawing I0038D01 of a counter-wound solenoid with the same design philosophy 6.25" diameter by 2.625" long. The MFA magnets have this envelope and are likely represented by the drawing.

If other drawings are found, they will be modeled.

Existing counter-wound solenoids

The figure on the next page shows an exploded view of the solenoid which I believe is placed around the chopping slits. The chopping circle is 3cm diameter. The chopping slits are 24 degrees in theta and +/-0.3cm in radial extent. The center of the B slit is at (0,1.5) in the coordinate system used for all these models. Since the models are axisymmetric, I evaluate fields only in the B slit. Drawing I0038D01 is identical in design philosophy with reduced dimensions as mentioned above. It fits over 1.5" beam pipe rather than the 2.5" shown.

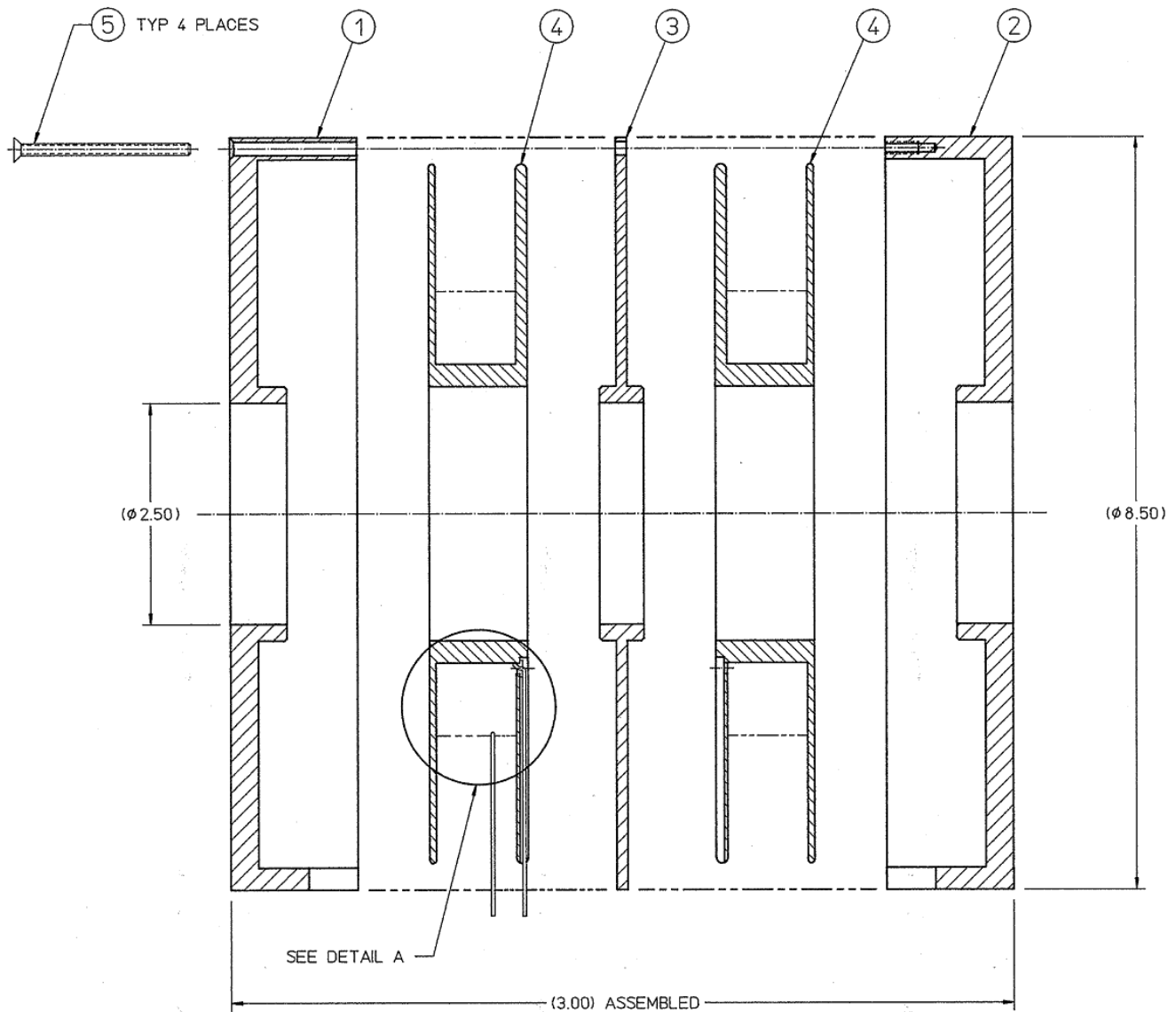
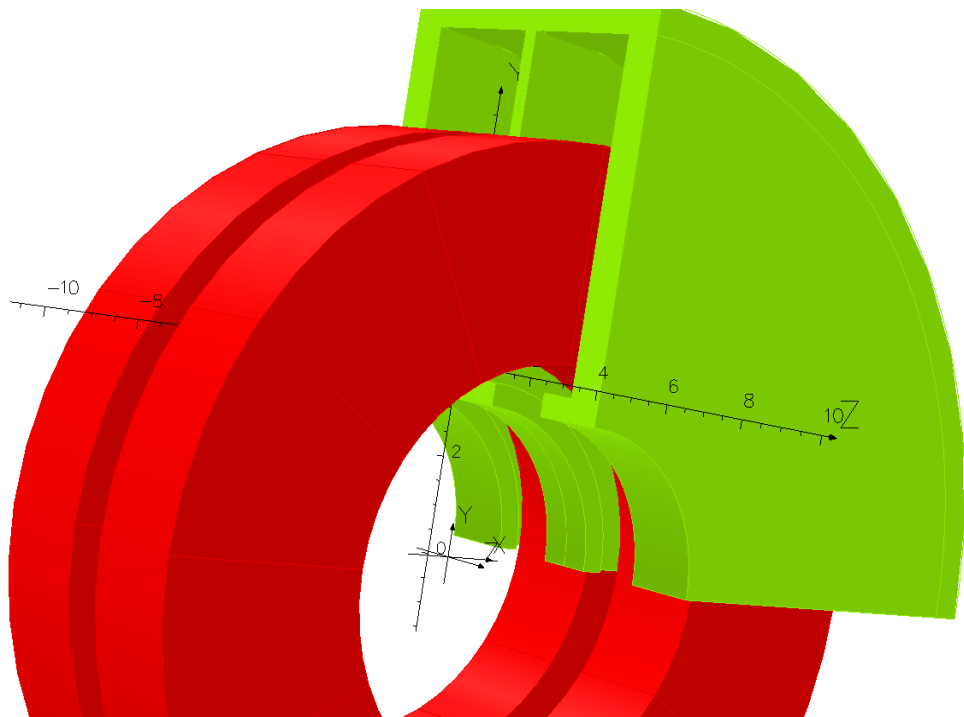


Figure 1 is taken from a pdf of the “injector solenoid” drawing from JLab Document Control which has the correct envelope. It shows an exploded view of the assembly. Note that the steel extends well under the coils at both the center (4.76mm) and at the end (8.31mm). This likely was done to reduce the field outside the end plate. That in turn may have been desired to make it easier to model the beam line with independent elements rather than elements with overlapping fields. Yet the beam line layout is such that solenoids are far enough apart that overlapping fields aren't an issue except in two locations (next paragraph). There are air core correctors close to the solenoids, but stray B_z fields won't matter to those and they aren't turned on in the models. The steel extensions are far longer than needed to orient the coil formers and would be symmetric about the coil centers if that was their only purpose.

Two MFA magnets, 6.25” diameter by 2.625” long, are butted up against the entrance of chopper cavity one and exit of chopper cavity two. These magnets are so close to the cavities that stray field is an issue for electron motion within the RF cavity. If one insists on having the magnets so close to the cavity rather than using a longer focal length, stray field reduction must be the highest priority. This is not the case for any other such units in the injector.



Opera

Figure 2 is a model in which the rotational symmetry is such that only a fourth of the elements are calculated. It shows how the steel comes under the coils asymmetrically in Z. The coil extends $z=[.489,2.808]$ so the coil center is $z=1.65\text{cm}$.

Finding the gradients in the counter-wound solenoid disheartening and having decided that a much shorter shoulder would suffice to locate the coil formers radially, I reduced the two shoulders from 4.76mm and 8.31mm to 1mm each in the model and solved again. Were these solenoids not welded onto the beam line by the vacuum flanges it would be easy to disassemble them, machine down the shoulders, and reassemble. Since these coils have never seen more than 200 keV beam, activation isn't an issue.

I then iterated these models, adjusting the current to get constant B_z^2 at $(0, 1.5, z)$. In table 1 I compare the $B_z \cdot dL$ and $B_z^2 \cdot dl$ integrals for $z=[0,10]\text{cm}$ for two models of the 8.5" counterwound solenoid and two models of the 6.25" counterwound solenoid, as designed and with shoulders machined. After the table I provide plots of B_z vs z and B_z^2 vs z for the models so the stray field may be examined. All of these are plotted only for the positive half of the models. These are plotted at the B hole center, $(0, 1.5, z)$. A and C hole centers are at $(+1.3, -0.752)$ in the coordinate system used in all the models shown.

1mm mesh with quadratic interpolation was used inside 3.18cm radius in the larger solenoid and 1.5cm radius in the smaller solenoid, extending to $z=10\text{cm}$. 2 mm quadratic mesh was used in the steel and air containing the coils. Coarser linear meshes are used outside these regions, graded from 4mm to 8mm and finally 10cm for the far field.

Table 1. Comparison of four models (magnitudes)

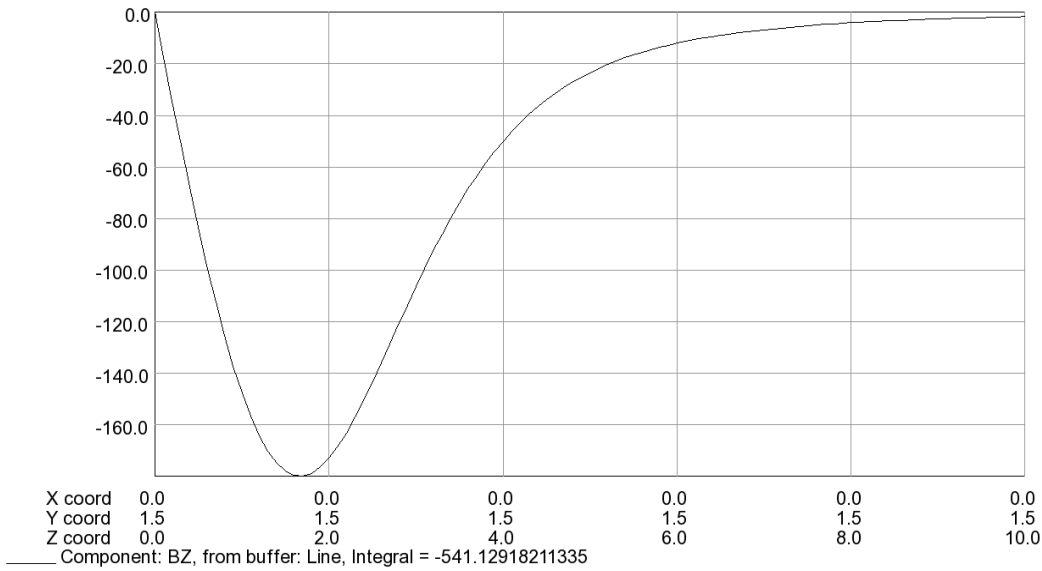
z_runs_0_to_10cm	8.5in_cntwnd	8.5in_cntrwd_mach	6.25in_cntrwd	6.25in_cntrwd_mach
Bz_dl_(0,1.2,z)	513.44	544.79		
Bz_dl_(0,1.5,z)	541.13	569.23		
Bz_dl_(0,1.8,z)	578.2	601.79		
Bz_dl_(0,0,z)			416.5	443
Bz_dl_(0,0.5,z)			429.9	454.23
G/cm	107.93	95.00	26.8	22.46
fraction_of_installed		0.880		0.838
Bz*Bz_dl(0,1.2,z)	56181.23	57914.06		
Bz*Bz_dl(0,1.5,z)	66169.92	66145.83		
Bz*Bz_dl(0,1.8,z)	81653.52	78324.55		
Bz*Bz_dl_(0,0,z)			52411.4	52414.59
Bz*Bz_dl_(0,0.5,z)			57942.2	56507.47
G^2/cm	42453.82	34017.48	11061.6	8185.76
fraction_of_installed		0.801		0.740

The upper half of the table shows BdL integrals. For the 8.5” solenoids the values are given at the bottom (1.2), middle (1.5) and top (1.8) of the hall B chopping slit hole. For the 6.25” solenoids the values are given at the center and at a radius of 0.5cm as the beam is nominally centered in these magnets. The “mach” solenoids have the steel shoulders machined down to 1mm, just enough to locate the coil formers, in the models. This reduces the gradient modestly and the difference in focusing strength more, as shown on the “fraction of installed” lines. The bottom half of the table has Bz² values. As mentioned on the previous page, the currents in the models were adjusted to maintain constant focusing at the nominal radius of use, 1.5cm for the 8.5” solenoids and 0 for the 6.25” solenoids. The focusing for the 8.5” solenoid is that produced by 0.758A, the value in the May 17 allsave. The smaller solenoid is used at various currents in the injector so 1A was used in the as-installed model and 1.0563A in the “machined” model to match the focusing.

108 G/cm is 1.08 T/m. This is a very high gradient for a 100 or 130 keV beam. The focusing strength is 15% lower at the bottom of the slit and 23% higher at the top of the slit than it is at the center. If the beam is not precisely axial going into the chopper cavity the three bunches will be at different radii as they encounter the magnets before and after the chopping slit assembly and will be focused differently. This difference will propagate through the rest of the machine because it can be dealt with only where the beams are separated, in the hall lines.

As shown in figure 2, there is a lot of radial room available for coil within the steel shell. The hole in the steel end plates was sized to locate the magnet on the beam pipe, 1.5” or 2.5”. A design with the same envelope is possible with higher homogeneity. One simply moves the coil and the steel ID outwards. One can maintain the use of the end plate ID as datum for solenoid location via an interference fit of an aluminum insert. Cool the aluminum down with LN2, pop it into place, and let it warm up. Stray field will increase but that's a much smaller issue than the radial gradients shown. Such models are discussed in the next section. Current will be higher if the #18 round conductor is maintained, but there's lots of room for water cooling at the inner diameter if needed. I use #14 square conductor in my designs so actual current density will be higher and current doesn't go up too much.

15/Nov/2012 14:10:52



UNITS
 Length cm
 Magn Flux Density gauss
 Magnetic Field oersted
 Magn Scalar Pot oersted cm
 Current Density A/cm²
 Power W
 Force N

MODEL DATA
 chopper_sol_counter_full_R2mod100.op3
 TOSCA Magnetostatic
 Nonlinear materials
 Simulation No 2 of 2
 12194430 elements
 11599329 nodes
 2 conductors
 Nodally interpolated fields
 Activated in global coordinates

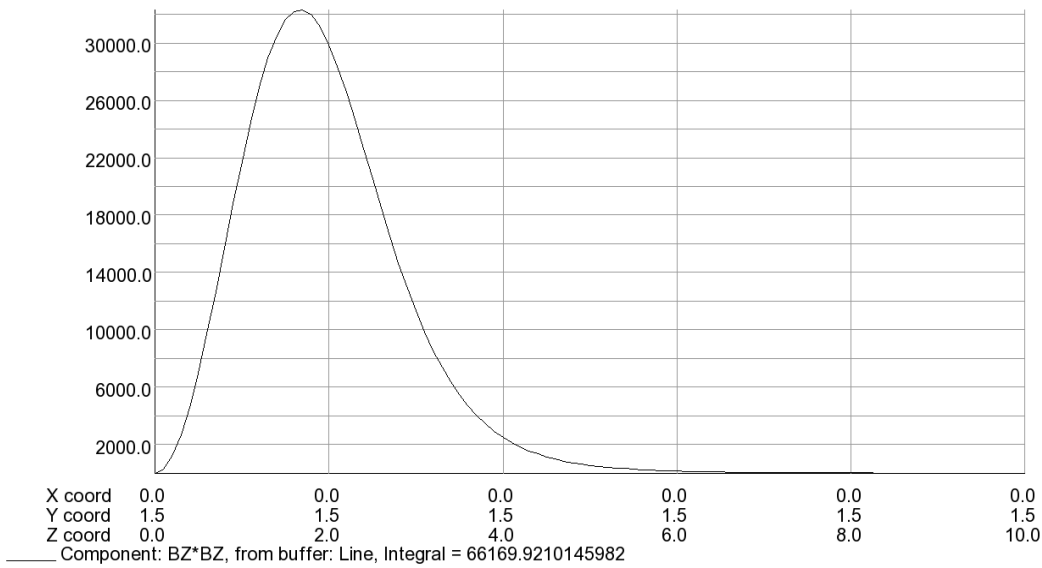
Field Point Local Coordinates
 Local = Global

FIELD EVALUATIONS
 Line LINE (nodal) 101 Cartesian
 x=0.0 y=0.0 z=0.0

Opera

Figure 3. $B_z(0,1.5,z)$ for 8.5" counter-wound solenoid with deep shoulders. I have the positive current coil first in the pair, in negative Z, and that coil forces the field to zero at $Z=0$.

15/Nov/2012 14:11:16



UNITS
 Length cm
 Magn Flux Density gauss
 Magnetic Field oersted
 Magn Scalar Pot oersted cm
 Current Density A/cm²
 Power W
 Force N

MODEL DATA
 chopper_sol_counter_full_R2mod100.op3
 TOSCA Magnetostatic
 Nonlinear materials
 Simulation No 2 of 2
 12194430 elements
 11599329 nodes
 2 conductors
 Nodally interpolated fields
 Activated in global coordinates

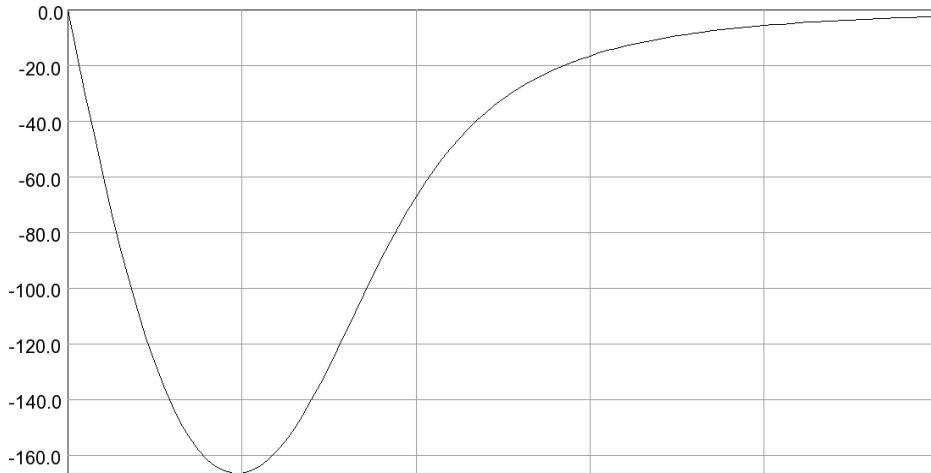
Field Point Local Coordinates
 Local = Global

FIELD EVALUATIONS
 Line LINE (nodal) 101 Cartesian
 x=0.0 y=0.0 z=0.0

Opera

Figure 4. $B_z(0,1.5,z)*B_z(0,1.5,z)$ for counter-wound solenoid with deep shoulders

15/Nov/2012 14:13:40



X coord	0.0	0.0	0.0	0.0	0.0	0.0
Y coord	1.5	1.5	1.5	1.5	1.5	1.5
Z coord	0.0	2.0	4.0	6.0	8.0	10.0

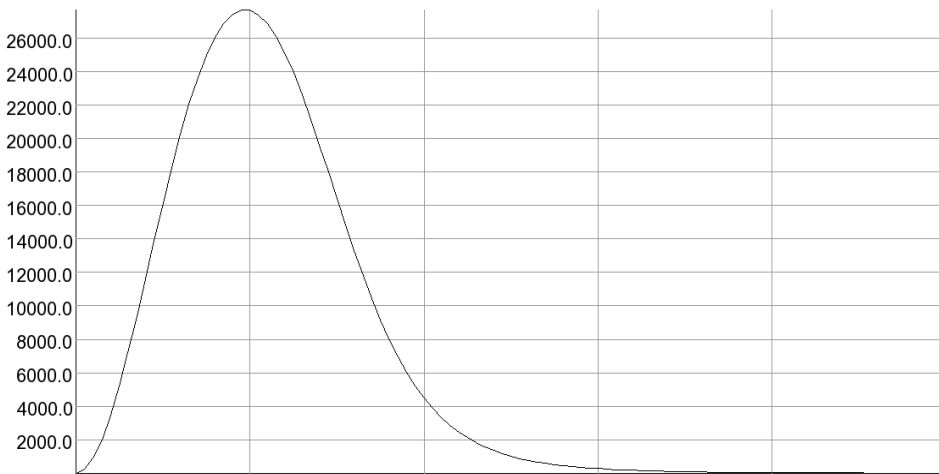
Component: BZ, from buffer: Line, Integral = -569.230411033029

UNITS	
Length	cm
Magn Flux Density	gauss
Magnetic Field	oersted
Magn Scalar Pot	oersted cm
Current Density	A/cm ²
Power	W
Force	N
MODEL DATA	
chopper_sol_cntr_full_R4_lip_mod100.op3	
TOSCA Magnetostatic	
Nonlinear materials	
Simulation No 2 of 2	
12092590 elements	
11460513 nodes	
2 conductors	
Nodally interpolated fields	
Activated in global coordinates	
Field Point Local Coordinates	
Local = Global	
FIELD EVALUATIONS	
Line LINE (nodal) 101 Cartesian	
x=0.0	y=0.0 z=0.0

Opera

Figure 5. $B_z(0,1.5,z)$ for counter-wound solenoid with narrow shoulders. Note that the peak magnetic field has moved out in Z vs figure 3 and is lower in amplitude. This is due to the steel shoulders. Stray field has increased.

15/Nov/2012 14:13:13



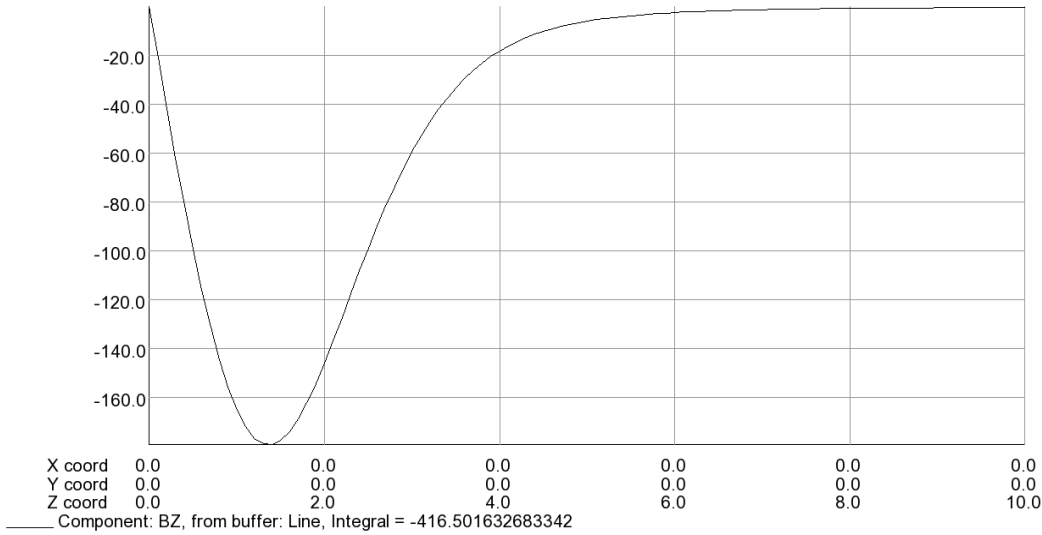
X coord	0.0	0.0	0.0	0.0	0.0	0.0
Y coord	1.5	1.5	1.5	1.5	1.5	1.5
Z coord	0.0	2.0	4.0	6.0	8.0	10.0

Component: BZ*BZ, from buffer: Line, Integral = 66145.8313229884

UNITS	
Length	cm
Magn Flux Density	gauss
Magnetic Field	oersted
Magn Scalar Pot	oersted cm
Current Density	A/cm ²
Power	W
Force	N
MODEL DATA	
chopper_sol_cntr_full_R4_lip_mod100.op3	
TOSCA Magnetostatic	
Nonlinear materials	
Simulation No 2 of 2	
12092590 elements	
11460513 nodes	
2 conductors	
Nodally interpolated fields	
Activated in global coordinates	
Field Point Local Coordinates	
Local = Global	
FIELD EVALUATIONS	
Line LINE (nodal) 101 Cartesian	
x=0.0	y=0.0 z=0.0

Opera

Figure 6. $B_z(0,1.5,z) \cdot B_z(0,1.5,z)$ for counter-wound solenoid with narrow shoulders



UNITS
 Length cm
 Magn Flux Density gauss
 Magnetic Field oersted
 Magn Scalar Pot oersted cm
 Current Density A/cm²
 Power W
 Force N

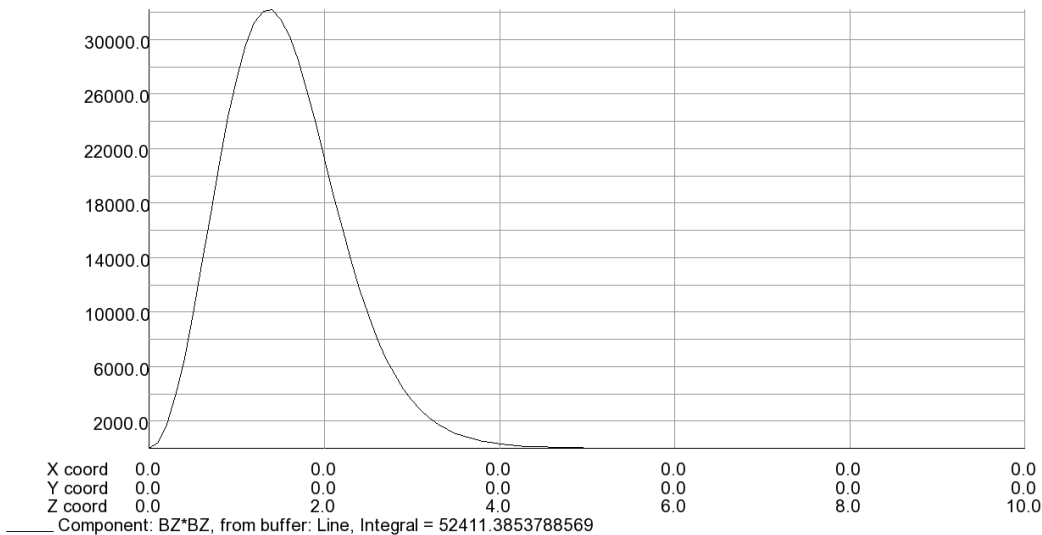
MODEL DATA
 inj_sml_cntr.op3
 TOSCA Magnetostatic
 Nonlinear materials
 Simulation No 1 of 1
 13770052 elements
 13815866 nodes
 2 conductors
 Nodally interpolated fields
 Activated in global coordinates

Field Point Local Coordinates
 Local = Global

FIELD EVALUATIONS
 Line LINE (nodal) 101 Cartesian
 x=0.0 y=0.0 z=0.0

Opera

Figure 7. “MFA” magnet Bz along centerline showing Bz=18G at z=4cm and 6G at 5cm versus peak of 179G. The envelope of this model is 6.25” diameter by 2.625” long.



UNITS
 Length cm
 Magn Flux Density gauss
 Magnetic Field oersted
 Magn Scalar Pot oersted cm
 Current Density A/cm²
 Power W
 Force N

MODEL DATA
 inj_sml_cntr.op3
 TOSCA Magnetostatic
 Nonlinear materials
 Simulation No 1 of 1
 13770052 elements
 13815866 nodes
 2 conductors
 Nodally interpolated fields
 Activated in global coordinates

Field Point Local Coordinates
 Local = Global

FIELD EVALUATIONS
 Line LINE (nodal) 101 Cartesian
 x=0.0 y=0.0 z=0.0

Opera

Figure 8. Bz*Bz for the same magnet. The integral of the tail beginning at z=3.8cm is 1% of the total. This z is 0.5cm beyond the magnet case. Bz(0,0,3.8)=23G. Very low stray field for a 1.5” hole.

If stray field is the primary concern; one is using 2mm apertures to trim the beam early in the injector; and the nuclear physics experiments that one is trying to serve are looking at large physics asymmetries, these are fine magnets. If the asymmetries are ~250ppb as in Qweak or ~35ppb as in the proposed MOLLER experiment, micron-level steering by the Pockels cell will be turned into optics changes by the gradients in these counter-wound solenoids. The insertable half-wave plate changes will help null the physics result of these, but reducing the effect of steering changes on optics is always desirable.

Alternate design 1: simple solenoid

The chopper is after the Wien filters so counter-wound solenoids are used in its vicinity. Since there are a pair of nominally identical solenoids placed on either side of the chopping slits with centers ~26cm apart it is not clear that the use of counter-wound solenoids is necessary: the pair of solenoids may be powered in series with opposite signs to provide zero net precession. The two magnets are driven in series per EPICS. For GPT particle tracking the first model constructed was a simple solenoid as the author had not yet obtained the drawings discussed above. This is shown in figure 9. It is a peculiarity of Opera that full coils must be placed in models but steel and air can be handled with symmetry planes and only half placed explicitly.

9/Nov/2012 08:45:42

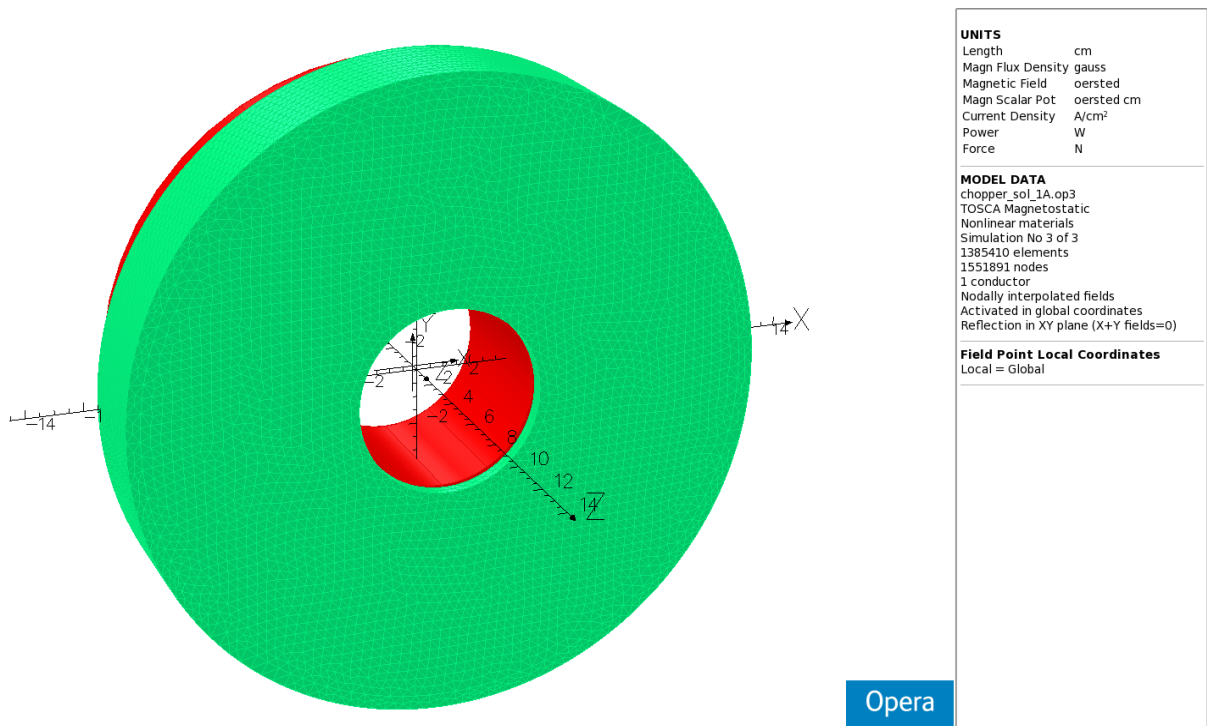
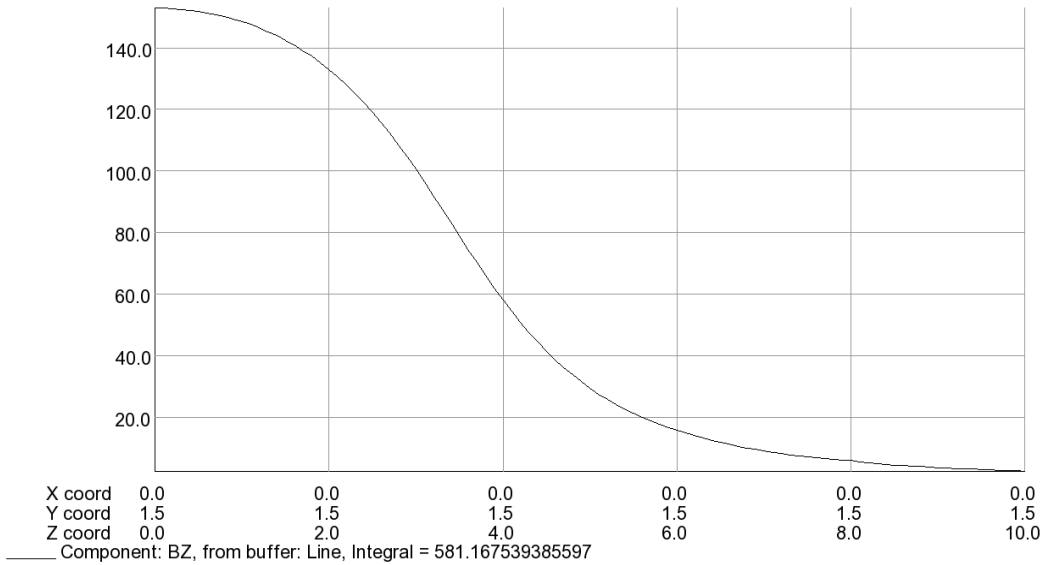


Figure 9. Simple solenoid model. 5 mm steel, 3mm Z gap and 4mm R gap between coil and steel. Similar envelope to existing MFD solenoids: 9" OD and 3" in Z, fitting over 2.5" tube. It's hard to measure the magnets in their recesses without a caliper and I got it wrong. The drawings arrived after this model was created.

The gradient across the chopping slit is only 0.7% of that shown in the second column of table 1, 0.8 G/cm here vs 108 G/cm in that model for the same nominal focusing strength, 66170 G² at y=1.5. However, the gradient in focusing strength, G²/cm, is ~6100/cm, 14.4% of the MFD. Per the OptiM model, the chopping slit is 13.2cm from the centerline of these magnets. Stray field isn't an issue with this gap, as seen in the next two figures. There was no problem propagating the beam through these solenoids in GPT. The beam didn't propagate through the field maps of the models described earlier in this paper without very high focusing on upstream magnets so the envelope function was already small when it encountered those units.

If the decision is taken to use simple solenoids around the chopper, I'll do a real engineering design, as I did for the next two magnets.



UNITS
 Length cm
 Magn Flux Density gauss
 Magnetic Field oersted
 Magn Scalar Pot oersted cm
 Current Density A/cm²
 Power W
 Force N

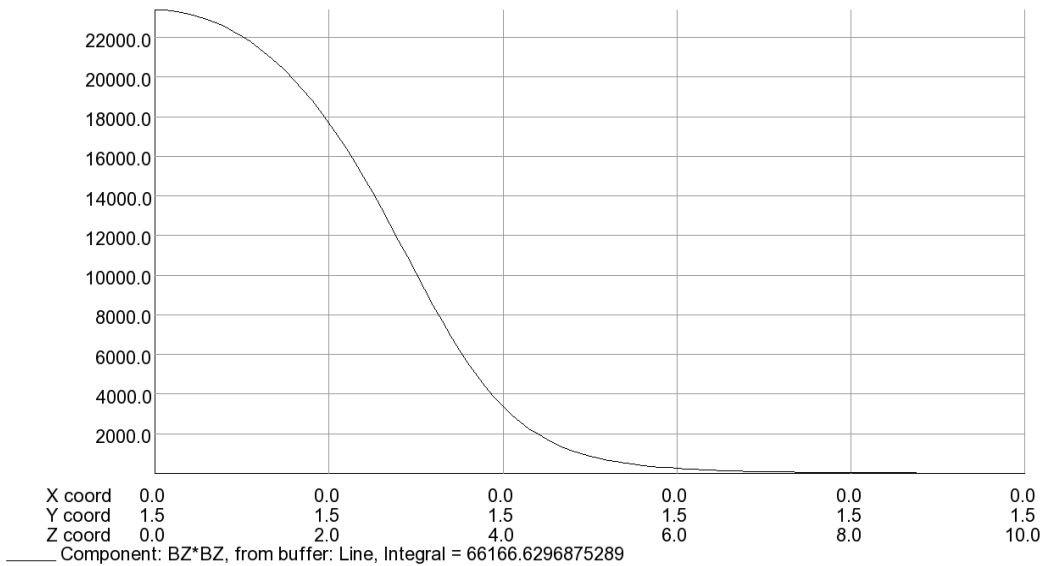
MODEL DATA
 chopper_sol_23_6A.op3
 TOSCA Magnetostatic
 Nonlinear materials
 Simulation No 2 of 2
 1385410 elements
 1551891 nodes
 1 conductor
 Nodally interpolated fields
 Activated in global coordinates
 Reflection in XY plane (X+Y fields=0)

Field Point Local Coordinates
 Local = Global

FIELD EVALUATIONS
 Line LINE (nodal) 101 Cartesian
 x=0.0 y=0.0 z=0.0

Opera

Figure 10. Bz for simple solenoid through the center of the B slit. Only the positive half of the field is shown so the Bz² value below is comparable to that in half a counter-wound unit. Bz(0,1.5,13.2), aka the center of the B slit in these coordinates if the OptiM model is correct, is 1G. Not a problem. The chopper cavity is considerably farther away from this magnet than is the slit.



UNITS
 Length cm
 Magn Flux Density gauss
 Magnetic Field oersted
 Magn Scalar Pot oersted cm
 Current Density A/cm²
 Power W
 Force N

MODEL DATA
 chopper_sol_23_6A.op3
 TOSCA Magnetostatic
 Nonlinear materials
 Simulation No 2 of 2
 1385410 elements
 1551891 nodes
 1 conductor
 Nodally interpolated fields
 Activated in global coordinates
 Reflection in XY plane (X+Y fields=0)

Field Point Local Coordinates
 Local = Global

FIELD EVALUATIONS
 Line LINE (nodal) 101 Cartesian
 x=0.0 y=0.0 z=0.0

Opera

Figure 11. Bz*Bz for simple solenoid along (0, 1.5, z). Integral of this z=[13.2,20] is a part in 20,000 of the total shown through 10cm. Again, not a problem.

This simple solenoid design should be considered as a replacement for the existing MFD magnets. This design has **not** been optimized for field quality. Steel and coil dimensions were chosen on the basis of the author's experience, not a parameter space search. See page 13 and appendices.

Two counter-wound designs with trade-off data

As discussed at the bottom of page 4, there is a substantial parameter space for counter-wound magnets available within the envelope 8.5" diameter by 3" length in the MFD magnets. This was explored. I began by looking at copper pipe sizes for the coil former. I settled on 4.5" OD by 4" ID. The outer shell is carbon steel mechanical tube, 8.5" OD with 0.25" wall. The copper sheet for the sides of the coil former and steel for the middle and ends then had to be chosen. I used 48 oz copper (1.6mm). For the end steel, 3mm, not quite 0.125". For the middle steel I used 2mm, thinking about galvanized sheet. This turned out to be too thin but I didn't revise the model for the parameter study. If this is built, 3.2mm (0.125") carbon steel for middle and ends. Conductor chosen was #14 square with single film insulation, the smallest available square wire in the old days. 18 turns wide, 24 layers, 432 turns total. So the Z profile from the center-line goes:

1mm steel
1.65mm copper (non-magnetic)
30.8mm coil
1.65mm copper
3mm steel

total 38.1mm, 1.5" With real steel, 0.8mm increase in half length, 3.06" total

I fixed the hole in the middle steel at 57.2 mm radius, the OD of the copper pipe, and varied the radius of the hole in the end steel from 32 to 71 mm in roughly uniform steps. The smallest corresponds to 2.5" beam pipe and the largest is limited by concerns about stray field – even I have them. The two plots that follow show the dependence of (integral Bz) variance across the chopper slit with end plate hole radius and that of (integral Bz²) with the same independent variable. These should be compared with the fourth and eighth numbers in column two of table one, 108 G/cm and 42454 G²/cm, for the (likely) installed magnet.

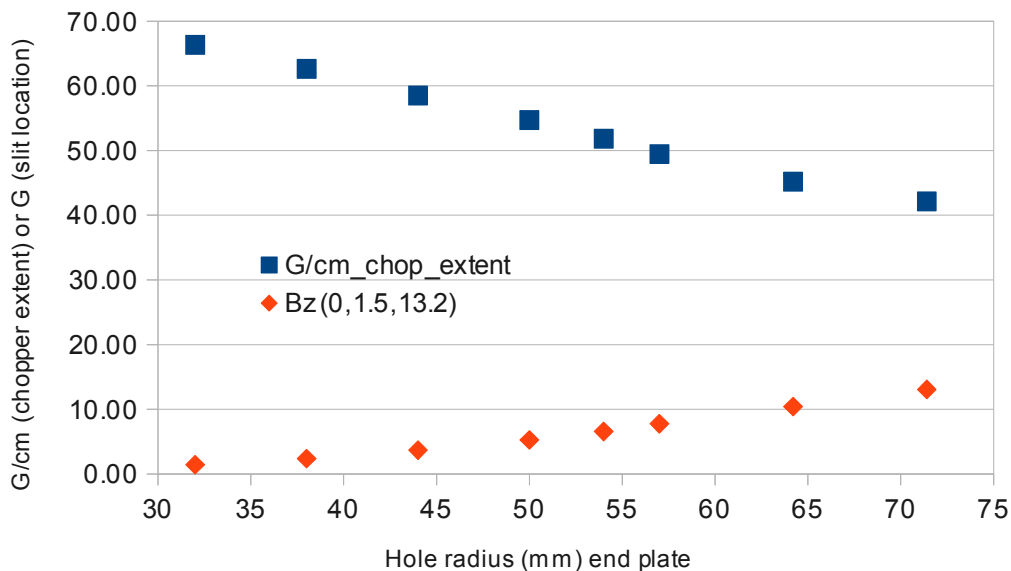


Figure 12. Dependence of gradient across the chopper slit radial extent and the field at the slit on the magnet steel end plate hole radius. The gradient is well below the 108 G/cm for the installed magnet even at at same (32mm) hole radius.

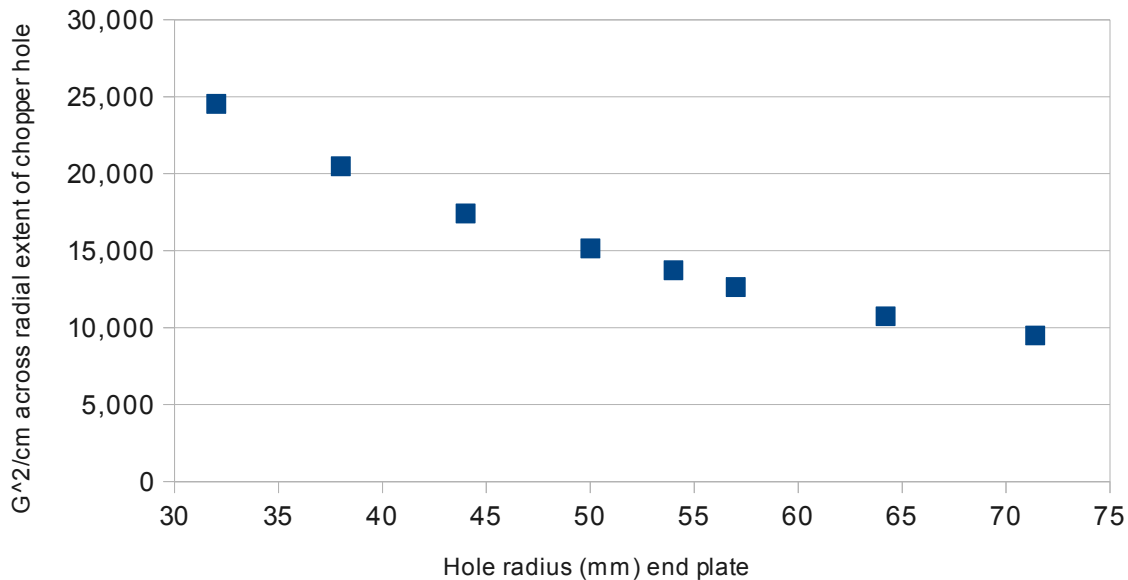


Figure 13. Dependence of the focusing strength difference across the radial extent of the chopper slit on the radius of the hole in the steel end plate of the counter-wound design which is 76.2mm long. This is parabolic. With just the first six points the parabola had a minimum at 71mm but adding the last two points moved the minimum out. Given the increase in stray field at the chopper location with radius (figure 12), I terminated the parameter scan. Again, the value is well below that of the installed magnet, 42454 G²/cm, at the same hole radius (32mm).

Power dissipation in a pair of counter-wound units (four coils) of this design goes from 100W with 50mm radius hole down to 80W with 71mm radius hole.

I visited the chopper again with my ruler. I determined that the unit could be lengthened to 10cm from 3" by using a narrower collet to lock it in place and using some of the free region beyond the ends of the flange bolts. Box wrench allowance provided. Using this additional space will allow yet lower gradients across the extent of the chopper slits. This stacks up: 1.6mm steel, 2.2mm copper, 40.8mm coil, 2.2 mm copper, 3.2mm steel from the centerline. Copper is now 64 oz sheet and steel is 0.125". 50mm half-length. 24X24 turns of #14 square wire, increasing the resistance to 1.9 ohms/coil. With one old trim card driving both units one can obtain only about twice the old focusing strength due to the card's voltage limit. If two cards or a new trim supply are used, no problem with much higher focusing even without adding water cooling to the ID of the magnet, in the 0.75" annulus between a 2.5" OD beam pipe and the 4" ID copper coil former. With the one-third increase in turns lowering the current for same integrals, power dissipation is about half that in the 3" long design for fixed focusing strength.

With the results in figures 12 and 13 in mind, I modeled only hole radii of 50, 57, 64 and 71 mm for this design. Results are shown in the next two figures.

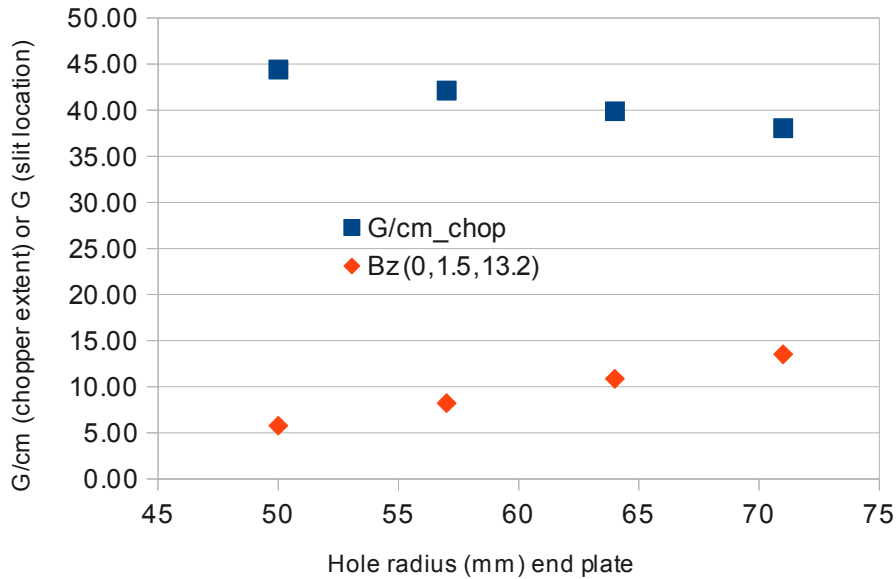


Figure 14. 10cm long counter-wound pair. Dependence of gradient across the chopper slit radial extent and the field at the slit on the magnet steel end plate hole radius. Gradient with 57mm radius hole is 85% of that in figure 12, the 3" long design. It's 39% of the installed unit.

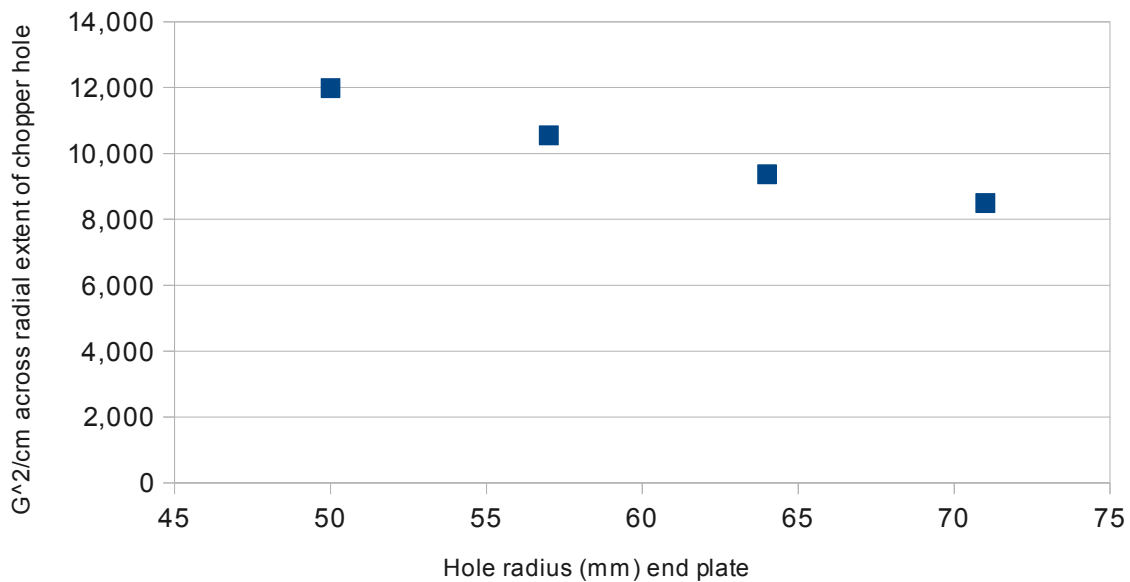


Figure 15. Dependence of the focusing strength difference across the radial extent of the chopper slit on the radius of the hole in the steel end plate of the counter-wound design which is 100mm long. For the 57mm hole, the value is 25% of the installed unit's.

More simple solenoid designs

After the counter-wound solenoid evaluation I went back to simple solenoids. I looked at the effect of steel end plate hole on my original solenoid and only then realized it was 9" OD. I did the hole end plate scan for a similar solenoid wound on at 2.5" nominal, 2.875" actual OD copper pipe. From there I examined a 77mm long solenoid on the same 4" nominal copper pipe used in the counter-wound designs. This provided better field uniformity at lower cost (less wire). Finally, I built a 97mm long solenoid to match the longer counter-wound. I foolishly didn't exactly match lengths but can go back and do so. This would reduce manufacturing costs via commonality of parts: simple and counter-wound solenoids built with exactly the same parts, the difference being only whether there was an central copper/steel/copper composite. Nevertheless, I present the results of the two simple solenoids of 4" copper ID in the appendix. In the table below I compare the four designs with the 57mm end hole to the magnet shown in figure 1, denoted MFD. If one prefers another hole size, see the appendices.

	MFD_model	57mm hole info			
		3"_counter	4"_counter	3"simple	4"simple
G/cm_chop	107.93	49.45	42.12	0.16	0.165
G/cm_center	14.34	7.14	6.56	0.028	0.028
G ² /cm_chop	42,454	12,637	10,548	2,969	2,349
G ² /cm_center	3965	1720	1497	455	367
Bz(0,1.5,13.2)	0.6	7.77	8.22	4.89	5.35
G ² fracMFD	1	0.298	0.248	0.070	0.055

Table 2. Comparing four solenoid design options to the modeled MFD. Two lengths, 3" and 4", and two winding patterns, simple and counter-wound. The lines labeled "chop" give gradients of integrated Bz or Bz² from r=1.8 cm to 1.2 cm. The lines labeled "cent" do the same for the central 0.5 cm radius circle. Bz(0,1.5,13.2) is the field at the chopper slit location in Optim in the coordinate system used in the models. The MFD design is an order of magnitude better on this criterion and horrible on the ones which count optically. As table A1 shows, it is possible to get 1.4G stray field at the slit with 58% of the gradient. Taken together, tables A1 and A2 suggest that the longer counter-wound design would have about half the focusing gradient of the MFD with 32mm radius steel end plate holes.

2002 measurements

I stumbled onto a 2002 email from Robin Wines forwarding a Tommy Hiatt spreadsheet of measurements of FD magnets. The table below compares the measurements at 0.8A and 0.6A to my model runs at those currents. Clearly the BH curve used for the 1010 steel, derived from old SLAC values, is wrong. But not too wrong. I'll forward the email to anyone interested.

		FD002	FD002	FD001	FD001
Current	amps	0.8	0.6	0.8	0.6
Bdl	G-cm	6.86	6.765	8.635	9.7525
Bdl per half	G-cm	497.705	382.6825	-490	-375.4525
B ² dl	G ² -cm	91635	54311	91794	54516
model_half	G-cm	501.4	376	-501.4	-376
model	G ² -cm	95411	53676	95411	53676
model/meas	G-cm	1.0074	0.9825	1.0233	1.0015
model/meas	G ² -cm	1.0412	0.9883	1.0394	0.9846
model 0.8/0.6		1.3335			
meas 0.8/0.6		1.3006		1.3051	

MFL0107 modeling (August 2014)

Drawing 341311-0003 was found by Joe Grames. In TN-14-017 he discusses precession measurements of this solenoid which follows the capture cavity and focuses 500 keV KE beam. The solenoid is immediately after aperture 4, with 6 mm diameter. Joe's original draft TN includes a POISSON model which suggested an unusual number of turns. My TOSCA model was done in an attempt to resolve questions.

The magnet is wound with #17 wire. I assume heavy film insulation, 0.0488" maximum diameter. The 1.04" bobbin width yields 21 turns/layer level wind and alternating 21 and 20 turn layers for hexagonal close pack winding. Joe's results suggested 698 +/- 2% turns. A hex close pack winding with 697 turns would have 3.692 cm radial extent, so this was used in the model. If the number of turns was instead 635 +/- 2%, as suggested by the TOSCA results and precession data, a level winding with 30 layers (630T) would be 0.09 cm thicker, irrelevant to the model accuracy. A 1010 carbon steel BH curve provided by VF with known errors (SLAC publication rounding issues) was modified and has been used in multiple TOSCA models by me, including this one. The drawing specifies 1006, 1008 or 1018 steel. The first two would give a bit better result and the last poorer than 1010.

The focusing term Bz^2 integrated over $z=[-15,15]$ is 648281 $G^2\text{-cm}$ at $y=0$ and 3.33% higher, 669876 $G^2\text{-cm}$, at $y=0.3$ cm, the top of the 6 mm diameter aperture 4. At 5 mm radius, which can't be reached unless the orbit is very extreme through A3 and A4, the focusing is 11.8% higher than at the center-line of the solenoid.

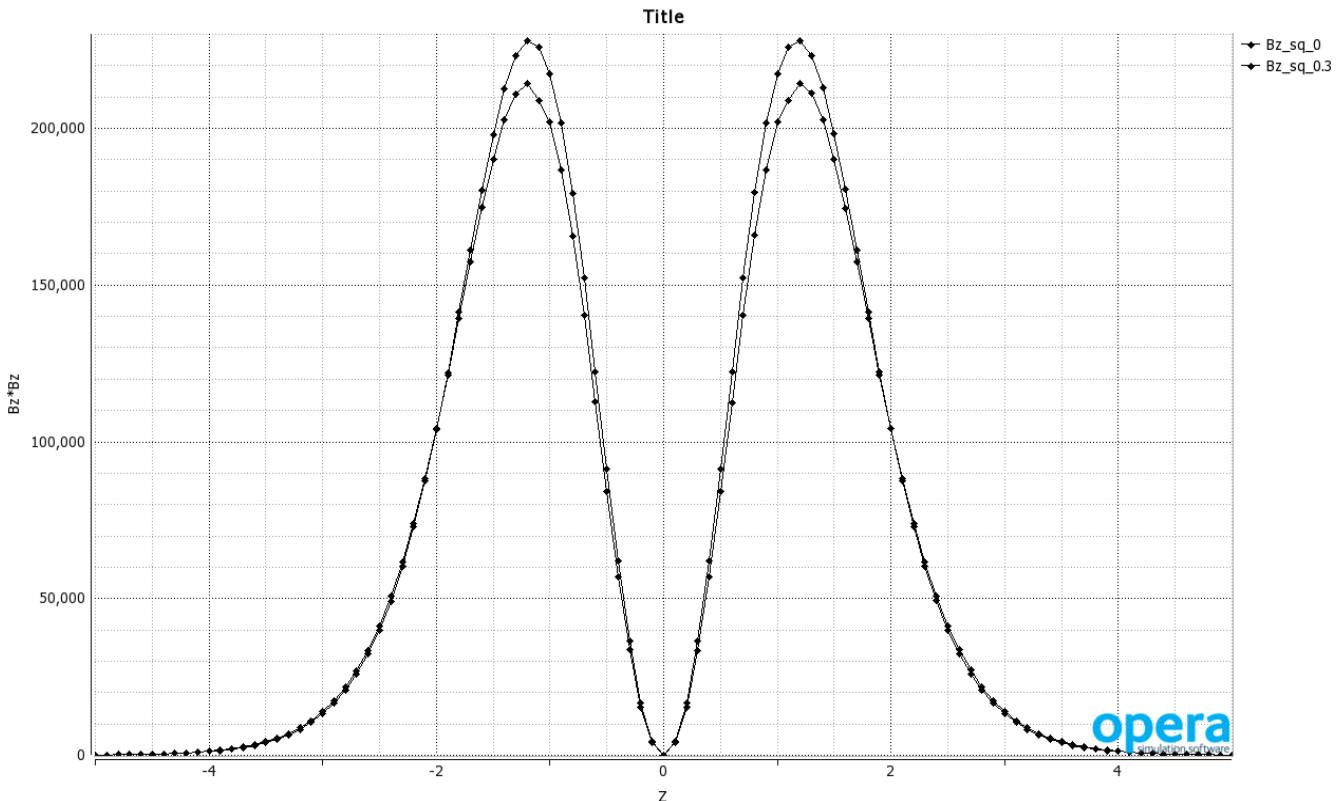
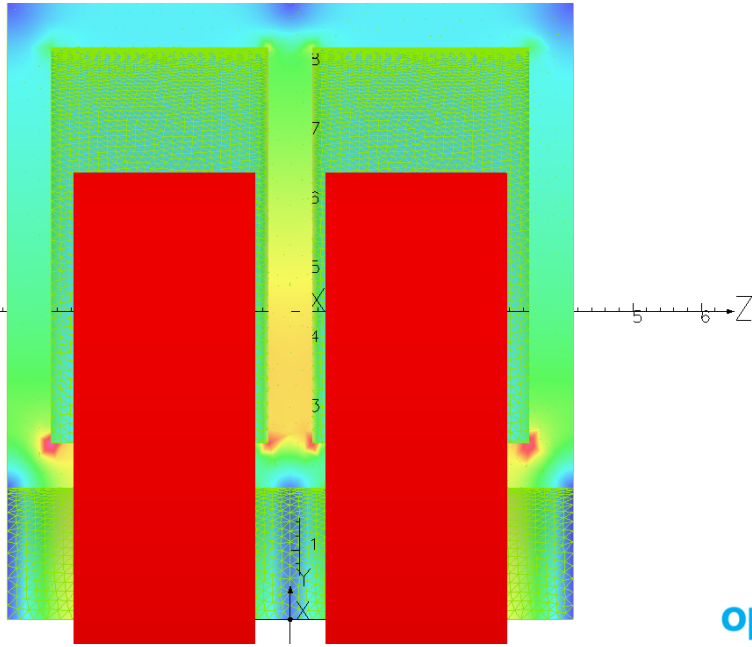
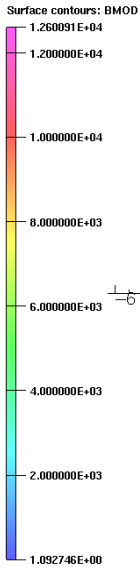


Figure 16. Bz^2 along lines at $y=0$ (lower) and $y=0.3$ cm (upper). Mesh is 2 mm with quadratic interpolation so 1mm point spacing was chosen for plot. If finer detail is required, the mesh size may be cut in half, increasing model size roughly a factor of eight.

24/Aug/2014 09:20:48

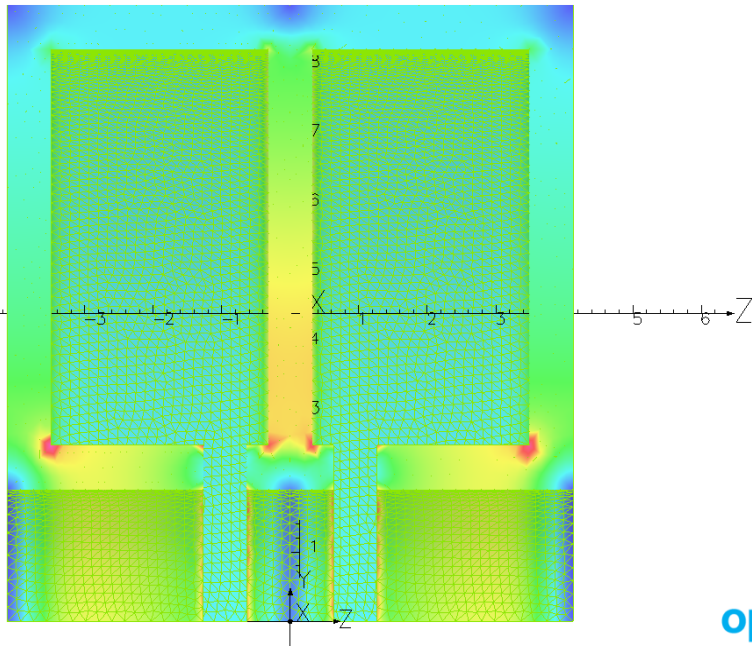
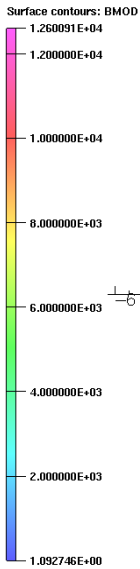


UNITS	
Length	cm
Magn Flux Density	gauss
Magnetic Field	oersted
Magn Scalar Pot	oersted cm
Current Density	A/cm ²
Power	W
Force	N
MODEL DATA	
MFJ_1163_quar_try1.op3	
Magnetostatic (TOSCA)	
Nonlinear materials	
Simulation No 2 of 3	
1946578 elements	
2669761 nodes	
2 conductors	
Nodally interpolated fields	
Activated in global coordinates	
4-fold rotational symmetry	
Field Point Local Coordinates	
Local = Global	
FIELD EVALUATIONS	
Line LINE	301 Cartesian
(nodal)	
x=0.0	y=0.5 z=-15.0 to 15.0



Figure 17 shows the MFL magnet modeled in TOSCA. The coil is slightly offset in the iron because the drawn tolerances allow this and the assembly process seemed likely to produce this result. Colors show peak field on the surface of the model in Gauss. Model was run with 2.24A (from allsave) in 630 turns vs 635 deduced from precession measurement.

24/Aug/2014 09:21:17



UNITS	
Length	cm
Magn Flux Density	gauss
Magnetic Field	oersted
Magn Scalar Pot	oersted cm
Current Density	A/cm ²
Power	W
Force	N
MODEL DATA	
MFJ_1163_quar_try1.op3	
Magnetostatic (TOSCA)	
Nonlinear materials	
Simulation No 2 of 3	
1946578 elements	
2669761 nodes	
2 conductors	
Nodally interpolated fields	
Activated in global coordinates	
4-fold rotational symmetry	
Field Point Local Coordinates	
Local = Global	
FIELD EVALUATIONS	
Line LINE	301 Cartesian
(nodal)	
x=0.0	y=0.5 z=-15.0 to 15.0



Figure 18. Same as above with coil hidden. One can see here how narrow (0.25") is the gap in the steel through which all the flux must penetrate to the bore. This small gap, less than half that in the MFA and MFD designs, is what drives the high gradient in focusing. The field is high in the central iron because the radial return flux for both coils passes through it in the same direction.

The MFL design makes even less sense to me than the MFA and MFD designs. The stray field in MFA and MFD is comparable to that in the MFL, less than 1% of peak 2 cm from steel face. Why close the gap for flux penetration even more here than the others?

Conclusions

I recommend that serious consideration be given to:

- a. replacing the simple solenoids in the front of the injector with one of the two designs presented here, reducing focusing variations across the bunch an order of magnitude.
- b. replacing all the counter-wound solenoids with one of the two designs presented where the increase in stray field is allowable, i.e. everywhere except the MFAs welded to the chopper cavities. I suggest the 100mm long design with 57mm radius holes in the end plates as a reasonable compromise between field quality and stray field. The MFAs could be replaced as well by exchanging locations with adjacent corrector set, reducing stray field within chopper cavity. Or, if one believes in superposition, one could maintain present location.

If not done during the long 12 GeV shutdown this should be considered again when the injector is upgraded to 200+ keV. We are going to have to learn to run that new injector from the models, so why not improve the magnets?

Footnotes

1.GPT General Particle Tracer from <http://www.pulsar.nl/index.htm>

Two sources which everyone doing solenoid magnet design should read:

Garrett, Milan Wayne, *Journal of Applied Physics* volume 38, pages 2563-2586 “Thick Cylindrical Coil Systems for Strong Magnetic Fields with Field or Gradient Homogeneities of the 6th to 20th Order” http://ieeexplore.ieee.org/xpls/abs_all.jsp?arnumber=5092187&tag=1

Montgomery, D. Bruce and Weggel, Robert J. *Solenoid Magnet Design*, 1980 Robert E. Kreiger Publishing Company, New York.

I rescued JLab's copy of the latter when the library reduced its collection.

Notes after meeting December 4, 2012

After the meeting Geoff Krafft remembered that he and Mike Tiefenback has written a PAC 93 paper on the longitudinal dynamics of the chopper.

http://accelconf.web.cern.ch/AccelConf/p93/PDF/PAC1993_0426.PDF

Of more relevance to this work is a PAC 93 paper by Joe Bisognano and Hongxiu Liu, “Simultaneous cancellation of beam emittance and energy spread in the CEBAF nuclear physics injector chopping system” http://accelconf.web.cern.ch/AccelConf/p93/PDF/PAC1993_0512.PDF

This paper shows the cross-section of the assembled MFD magnet as figure 3, verifying my figure 1. Figure 4 of the paper shows that the MFD is energized as a counter-wound solenoid. The paper provides analytical and modeling justification for the lens strength and placement. It follows that counter-wound solenoids are needed in the chopper. This work shows their performance can be improved by a factor of four. The PAC 93 papers are written for a thermionic source with emittance filter apertures of 2mm. These were enlarged for the G0 experiment to 4mm for the first and either 4mm or 6mm for the second. It follows that lens gradients are more important now than in 1993.

Dave Douglas and Bob Legg tell me that the chopper lenses have to be counter-wound to avoid twisting the beam as well as deflecting it to the chopper circle. So mote it be.

Appendix

Table A1. Comparison of 76mm long counter-wound models with different end hole radii. I show gradients in G and G^2 both in the center of the magnet and at the chopper slit radii (12, 15, 18) so one can compare this design to the MFA as well as the MFD in Table 1. Focusing strength at the middle of the chopper slit is not exactly 66170 G^2/cm as in the MFD in table 1, but close enough for these comparisons. Steel response isn't quite linear because the central piece is only 2mm. Worst case field in this steel is 15kG. As mentioned several times, if built all the steel annuli will be 3.2mm/0.125", dropping the field in the steel below 9kG. If one wants a fully linear system with much wider focusing range, double the central steel thickness, resulting in a total length of 81mm or 3.2".

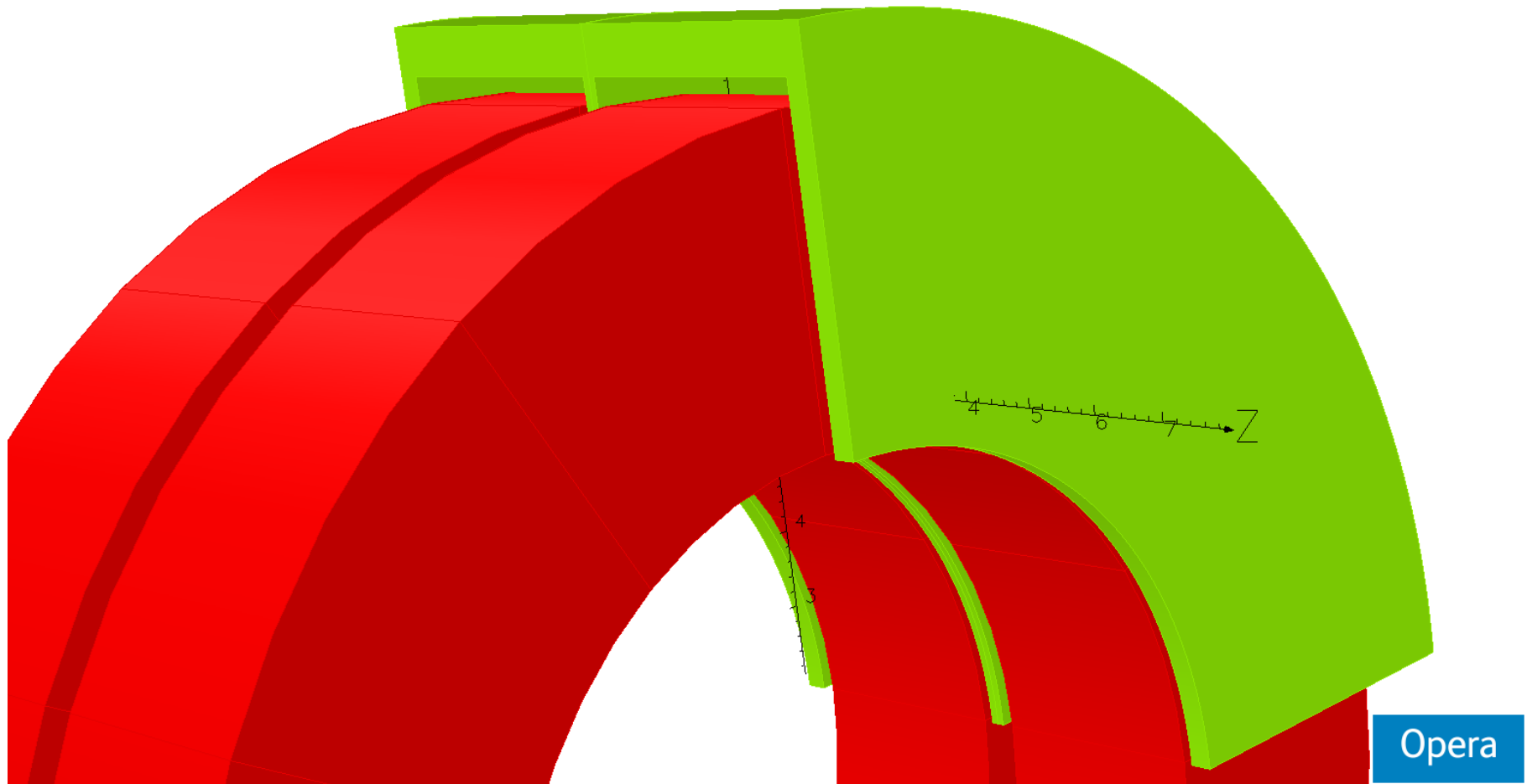
The integrals Bz_dl differ because the shape of the field differs with end plate hole. Fields with small holes in the steel are much more peaked in Z and so have high Bz^2 integrals with low Bz integrals.

z_runs_0_to_20cm	New_71_cntrv	New_64_cntrv	New_57_cntrv	New_54_cntrv	new_50_cntrv	New_44_cntrv	New_38_cntrv	New_32_cntrw
$Bz_dl(0,0,z)$	819.53	787.25	751.13	729.07	701.51	660.53	614.75	568.36
$Bz_dl(0,0.5,z)$	822.71	790.65	754.7	732.82	705.41	664.69	619.19	573.08
$Bz_dl(0,1.2,z)$	838.59	807.62	773.2	752.24	725.74	686.36	642.36	597.62
$Bz_dl(0,1.5,z)$	849.79	819.6	786.29	765.95	740.2	701.81	658.9	615.15
$Bz_dl(0,1.8,z)$	863.87	834.74	802.87	783.34	758.56	721.46	679.94	637.43
G/cm chop	42.13	45.20	49.45	51.83	54.7	58.5	62.63	66.35
frac_of_inst_MFD	0.390	0.419	0.458	0.480	0.507	0.542	0.580	0.615
G/cm center	6.36	6.8	7.14	7.5	7.8	8.32	8.88	9.44
frac_of_inst_MFA	0.237	0.254	0.266	0.280	0.291	0.310	0.331	0.352
$Bz(0,1.5,13.2)$	13.070	10.420	7.770	6.570	5.260	3.690	2.380	1.430
$Bz*Bz_dl(0,0,z)$	59599.1	58684.97	57993.2	57166.4	56076.5	54345.6	52341.3	50359.8
$Bz*Bz_dl(0,0.5,z)$	60272.1	59434.4	58853.1	58082.9	57074.7	55462.4	53608.5	51807.2
$Bz*Bz_dl(0,1.2,z)$	63650.6	63215.6	63231.3	62797.3	62209	61257.1	60258.3	59512.9
$Bz*Bz_dl(0,1.5,z)$	66121.2	66000.9	66490.3	66325.7	66087.1	65688	65425.4	65627.1
$Bz*Bz_dl(0,1.8,z)$	69345.3	69660.9	70813.5	71032.1	71299.4	71710.1	72554.3	74236.7
G^2/cm_chop	9,491	10,742	12,637	13,725	15,151	17,422	20,493	24,540
frac_of_inst_MFD	0.224	0.253	0.298	0.323	0.357	0.410	0.483	0.578
G^2/cm_center	1346	1498.86	1719.8	1833	1996.4	2233.6	2534.4	2894.8
frac_of_inst_MFA	0.122	0.136	0.155	0.166	0.180	0.202	0.229	0.262

Table A2. Comparison of 100mm long counter-wound models with different end hole radii. I show gradients in G and G^2 both in the center of the magnet and at the chopper slit radii (12, 15, 18) so one can compare this design to the MFA as well as the MFD in Table 1. Again, if one wants a magnet linear to over three times the field and ten times the focusing strength, double the central iron thickness to 6.35mm, increasing the overall length to 103.2mm. Power will be about 250W/unit so water cooling is then required.

A unit intermediate in length between those in A1 and A2 is also possible, of course, in units of 3.384mm. (Conductor width is 0.1692mm and one has to add or subtract from both coils, so $2*0.1692$.)

z_runs_0_to_20cm	10cm_71_cnt	10cm_64_cnt	10cm_57_cnt	10cm_50_cnt
Bz_dl_(0,0,z)	829.74	801.44	768.92	731.09
Bz_dl_(0,0.5,z)	832.77	804.55	772.2	734.54
Bz_dl_(0,1.2,z)	847.22	819.68	788.15	751.35
Bz_dl_(0,1.5,z)	857.34	830.28	799.34	763.15
Bz_dl_(0,1.8,z)	870.05	843.61	813.42	778
G/cm chop	38.05	39.88	42.12	44.42
frac_of_inst_MFD	0.353	0.370	0.390	0.412
G/cm center	6.06	6.22	6.56	6.9
frac_of_inst_MFA	0.226	0.232	0.245	0.257
Bz(0,1.5,13.2)	13.52	10.87	8.22	5.78
Bz*Bz_dl_(0,0,z)	60255.6	59602.2	58968.6	58005
Bz*Bz_dl_(0,0.5,z)	60872.4	60275.7	59717.3	58842.5
Bz*Bz_dl(0,1.2,z)	63941.3	63637.8	63470.8	63063.1
Bz*Bz_dl(0,1.5,z)	66163.4	66083.1	66216.5	66172.2
Bz*Bz_dl(0,1.8,z)	69036.8	69257.8	69799.7	70255.2
G^2/cm_chop	8,493	9,367	10,548	11,987
frac_of_inst_MFD	0.200	0.221	0.248	0.282
G^2/cm_center	1233.6	1347	1497.4	1675
frac_of_inst_MFA	0.112	0.122	0.135	0.151



Opera

Figure A1. Coils and steel for the 3" long counter-wound model with 57mm radius holes throughout. Note that the central steel is thinner (2mm) than the end steel (3mm) in this model. This will have to change to 3.2mm in all locations if this magnet is built. Or 6.35mm if one wants yet more linear range. Radial outward flux adds in the central plate from the two coils; it doesn't cancel.

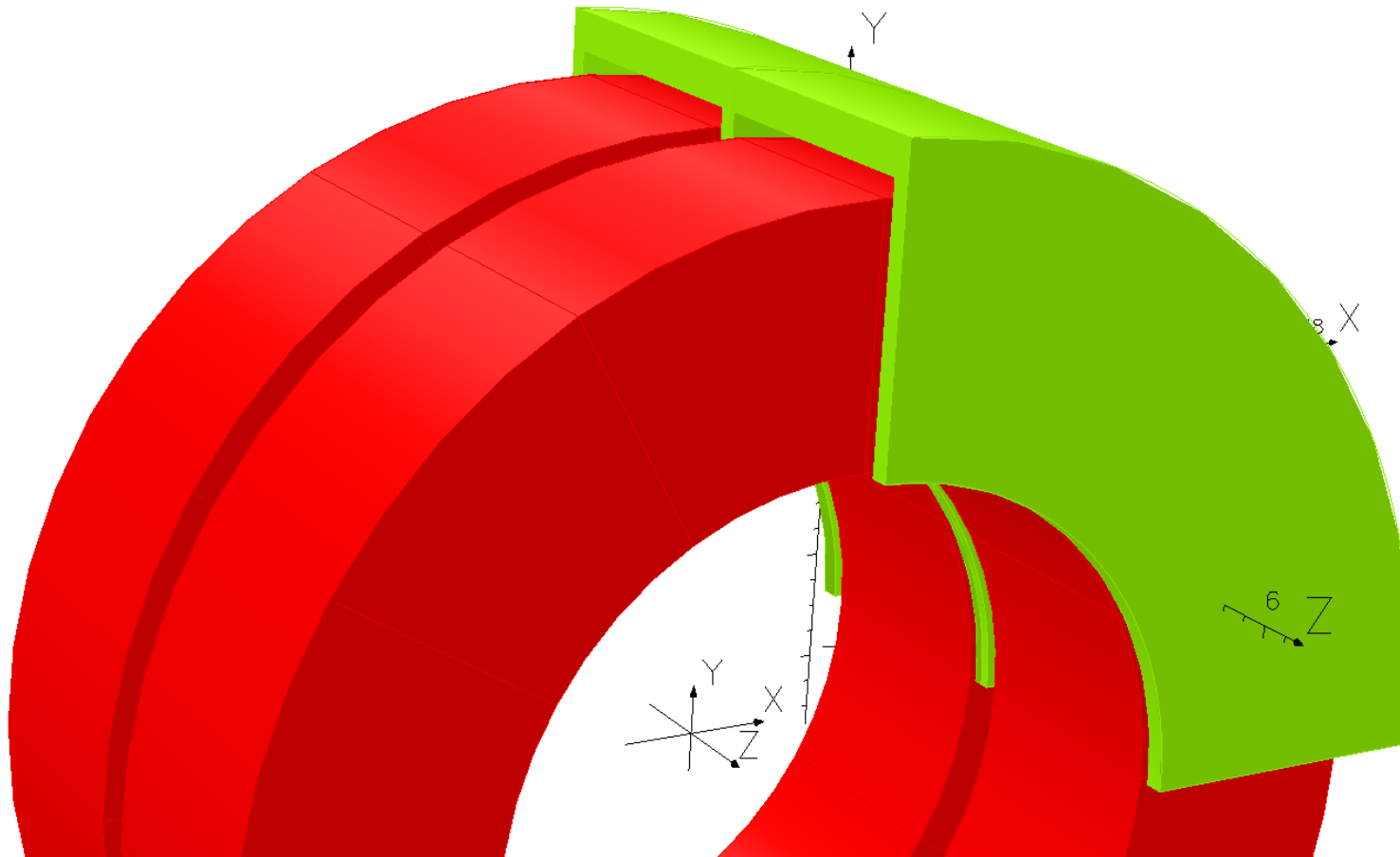


Figure A2. Coils and steel for the 10cm long counter-wound model with 57mm radius holes throughout. Steel is 3.2mm thick in all three plates. Again, to double the linear range, double the central steel thickness. And add water cooling to the bore.

Table A3. Performance of simple solenoid 74mm long. Current density for each model set to get close to the focusing of the Figure 1 magnet with the current in the May 17 allsave, 66170, bold below.

z_runs_0_to_20cm	71_coil_IR_bi	64_coil_IR_bi	61_coil_IR_bi	57_coil_IR_bi	50_coil_IR_bi
Bz_dl_(0,0,z)	785.86	756.96	742.885	723.682	688.586
Bz_dl_(0,0.5,z)	785.883	756.978	742.901	723.696	688.595
Bz_dl_(0,1.2,z)	785.995	757.064	742.997	723.759	688.6385
Bz_dl_(0,1.5,z)	786.071	757.123	743.029	723.801	688.668
Bz_dl_(0,1.8,z)	786.162	757.194	743.091	723.853	688.703
G/cm chop	0.28	0.22	0.16	0.16	0.107
frac_of_inst_MFD	0.003	0.002	0.001	0.001	0.001
G/cm center	0.046	0.036	0.032	0.028	0.018
frac_of_inst_MFA	0.002	0.001	0.001	0.001	0.001
Bz(0,1.5,13.2)	8.34	6.58	5.83	4.89	3.42
Bz*Bz_dl_(0,0,z)	64582.1	64354.5	64165.4	63973.7	63637.6
Bz*Bz_dl_(0,0.5,z)	64752.5	64549.6	64373.2	64201	63905.8
Bz*Bz_dl(0,1.2,z)	65580.9	65501	65387.97	65313	65223.7
Bz*Bz_dl(0,1.5,z)	66161.9	66170.7	66103.5	66099.3	66161.2
Bz*Bz_dl(0,1.8,z)	66891.6	67014.5	67006.7	67094.4	67354.3
G^2/cm_chop	2,185	2,523	2,698	2,969	3,551
frac_of_inst_MFD	0.051	0.059	0.064	0.070	0.084
G^2/cm_center	340.8	390.2	415.6	454.6	536.4

Table A4. Performance of simple solenoid 97mm long. Note that the hole sizes increase from left to right here. All previous tables have the largest hole, and therefore the lowest gradient, at the left. Current density for each model set to get close to the focusing of the Figure 1 magnet with the current in the May 17 allsave, 66170, bold below.

z_runs_0_to_20cm	97mmL_50mm	97mmL_57mm	97mmL_64mm	97mmL_71mm
Bz_dl_(0,0,z)	724.081	753.669	781.636	806.455
Bz_dl_(0,0.5,z)	724.091	753.683	781.655	806.48
Bz_dl_(0,1.2,z)	724.137	753.75	781.746	806.597
Bz_dl_(0,1.5,z)	724.168	753.795	781.807	806.676
Bz_dl_(0,1.8,z)	724.206	753.849	781.882	806.771
G/cm chop	0.115	0.165	0.227	0.29
frac_of_inst_MFD	0.001	0.002	0.002	0.003
G/cm center	0.02	0.028	0.038	0.05
frac_of_inst_MFA	0.001	0.001	0.001	0.002
Bz(0,1.5,13.2)	3.79	5.35	7.11	8.92
Bz*Bz_dl_(0,0,z)	64213	64453.5	64651.6	64773.3
Bz*Bz_dl_(0,0.5,z)	64422.4	64637	64813.7	64918.2
Bz*Bz_dl_(0,1.2,z)	65443.1	65528.8	65599.7	65619.8
Bz*Bz_dl_(0,1.5,z)	66161.6	66153.8	66148.7	66108.6
Bz*Bz_dl_(0,1.8,z)	67067.25	66938.1	66835.7	66719.1
G^2/cm_chop	2,707	2,349	2,060	1,832
frac_of_inst_MFD	0.064	0.055	0.049	0.043
G^2/cm_center	418.8	367	324.2	289.8